



Published in final edited form as:

Clin Neurophysiol. 2010 December ; 121(12): 2128–2133. doi:10.1016/j.clinph.2010.04.026.

Current-controlled deep brain stimulation reduces in vivo voltage fluctuations observed during voltage-controlled stimulation

Scott F. Lempka, M.S.^{1,2}, Matthew D. Johnson, Ph.D.¹, Svjetlana Miocinovic, M.D., Ph.D.^{1,2}, Jerrold L. Vitek, M.D., Ph.D.³, and Cameron C. McIntyre, Ph.D.^{1,2}

¹ Department of Biomedical Engineering, Cleveland Clinic Foundation, Cleveland, OH, U.S.A

² Department of Biomedical Engineering, Case Western Reserve University, Cleveland, OH, U.S.A

³ Department of Neurosciences, Cleveland Clinic Foundation, Cleveland, OH, U.S.A

Abstract

Objective—Clinical deep brain stimulation (DBS) systems typically utilize voltage-controlled stimulation and thus the voltage distribution generated in the brain can be affected by electrode impedance fluctuations. The goal of this study was to experimentally evaluate the theoretical advantages of using current-controlled pulse generators for DBS applications.

Methods—Time-dependent changes in the voltage distribution generated in the brain during voltage-controlled and current-controlled DBS were monitored with *in vivo* experimental recordings performed in non-human primates implanted with scaled-down clinical DBS electrodes.

Results—In the days following DBS lead implantation, electrode impedance progressively increased. Application of continuous stimulation through the DBS electrode produced a decrease in the electrode impedance in a time dependent manner, with the largest changes occurring within the first hour of stimulation. Over that time period, voltage-controlled stimuli exhibited an increase in the voltage magnitudes generated in the tissue near the DBS electrode, while current-controlled DBS showed minimal changes.

Conclusion—Large electrode impedance changes occur during DBS. During voltage-controlled stimulation, these impedance changes were significantly correlated with changes in the voltage distribution generated in the brain. However, these effects can be minimized with current-controlled stimulation.

Significance—The use of current-controlled DBS may help minimize time-dependent changes in therapeutic efficacy that can complicate patient programming when using voltage-controlled DBS.

Keywords

non-human primate; thalamus; subthalamic nucleus; globus pallidus; voltage-controlled stimulation; current-controlled stimulation

Corresponding author: Cameron C. McIntyre, Ph.D., Department of Biomedical Engineering, Cleveland Clinic Foundation, 9500 Euclid Ave., ND20, Cleveland, OH 44195, U.S.A., Phone: (216) 445-3264, Fax: (216) 444-9198, mcintyc@ccf.org.

Publisher's Disclaimer: This is a PDF file of an unedited manuscript that has been accepted for publication. As a service to our customers we are providing this early version of the manuscript. The manuscript will undergo copyediting, typesetting, and review of the resulting proof before it is published in its final citable form. Please note that during the production process errors may be discovered which could affect the content, and all legal disclaimers that apply to the journal pertain.

1. Introduction

Deep brain stimulation (DBS) is an established therapy for the treatment of movement disorders and shows promise for the treatment of several neuropsychiatric disorders (Perlmutter and Mink, 2006). Traditionally, clinical DBS systems have relied on voltage-controlled pulse generators; however, the recent introduction of current-controlled pulse generators has expanded the clinical options for DBS therapy. The use of voltage-controlled stimulation results in voltage distributions in the target neural tissues that depend upon the impedance of the electrode-tissue interface (Butson et al., 2006; Miocinovic et al., 2009). The impedance of the DBS electrode-tissue interface has been shown to fluctuate both after implantation and during stimulation (Lempka et al., 2009). These varying impedance conditions are suspected to produce instability in the voltages produced in the target neural tissues during voltage-controlled DBS, and may be at least partially responsible for the frequent need to adjust stimulation parameters during the initial patient programming process.

Unlike voltage-controlled DBS, current-controlled DBS regulates the current through the electrode-tissue interface. In theory, the voltages generated in the target brain tissues by current-controlled DBS should be fairly independent of the electrode impedance. This increased stability in the extracellular voltages produced from stimulation could help stabilize the therapeutic efficacy of stimulation parameters selected during patient programming. Therefore, we attempted to experimentally verify the theoretical advantage of current-controlled DBS relative to voltage-controlled DBS.

DBS was applied through leads implanted in rhesus macaque monkeys and the voltages in the surrounding neural tissue were monitored with microelectrode recordings. We first examined the temporal voltage fluctuations during voltage-controlled DBS, both after electrode implantation and during stimulation. Then we compared the magnitude of the voltage fluctuations that occur during voltage-controlled DBS relative to current-controlled DBS. Our results show that substantial voltage fluctuations occur within the first hour after activating a DBS electrode contact with voltage-controlled stimulation, but these fluctuations were minimized with current-controlled DBS. These results have important implications for clinical research analyses of the time-dependent wash-in behavioral effects of DBS, as well as for standard clinical DBS device programming.

2. Materials and Methods

2.1. Stimulation and recording protocols

The deep brain stimulation (DBS) electrodes used in this study were scaled-down versions of clinical DBS electrodes suitable for implantation in the brain of rhesus macaque monkeys (*Macaca mulatta*). The DBS leads were fabricated by Advanced Bionics Corporation (now Boston Scientific Neuromodulation, Valencia, CA) and each lead had a 45 mm polyurethane shaft with four cylindrical platinum/iridium contacts located near the distal end of the lead shaft. Each electrode contact was 0.75 mm in diameter and 0.5 mm height with 0.5 mm insulation separating individual contacts.

Both voltage-controlled and current-controlled stimulation were examined in this study. A voltage-controlled stimulus train ($-1.0V$ cathodic amplitude and $90\ \mu s$ pulses delivered at a frequency of 135Hz) was applied through a DBS contact using a clinical pulse generator (IPG; Itrel II model, Medtronic Inc., Minneapolis, MN) with the contralateral titanium access chamber as the return electrode (Fig. 1B). Current-controlled stimulation ($200\ \mu A$ amplitude and $90\ \mu s$ pulses delivered at a frequency of 135 Hz) was applied with an external pulse generator (S88; Grass Instruments, Quincy, MA) and two photoelectric constant-current stimulus isolation units (PSIU6, Grass Instruments) (Fig. 1B). The amplitude of the current-

controlled stimulus train was determined using current measurements during one of the aforementioned experiments utilizing voltage-controlled stimulation. The measured current typically varied between 100–300 μA in these experiments, and this variance was dependent on the DBS electrode impedance (data not shown). A 200 μA amplitude was thus selected for the current-controlled experiments.

The voltages generated in the brain during DBS were measured with differential recordings using an acutely implanted microelectrode. A guide tube was used to puncture the dura so that the recording microelectrode could be inserted with ~ 2 mm separation from the chronically-implanted DBS electrode using a microdrive (MO-95-1p, Narishige Scientific Instruments, Tokyo, Japan) (Fig. 1A). The stainless steel guide tube was placed a few millimeters below the dura and served as the reference electrode. Recordings were performed with both single-channel and multi-channel microelectrodes. Single-channel recordings were performed with epoxy-coated tungsten microelectrodes with tip lengths of approximately 50 μm (FHC, Bowdoinham, ME). The recorded signal was amplified ($50\times$) and band-pass filtered between 0.1 Hz and 20 kHz using a differential amplifier connected to a high-impedance headstage (model 3000, A-M Systems, Sequim, WA). The recorded signal was digitized at a sampling rate of 100 kHz and stored for offline analysis (Power 1401 and Spike2 software, Cambridge Electronic Design, Cambridge, UK). To increase the number of voltage recording locations, multi-channel recordings were performed in a subset of experiments using a linear array of 8 microelectrodes (NeuroNexus, Ann Arbor, MI). Recordings were sampled at 50 kHz through an Alpha-Lab system (Alpha Omega, Nazareth, Israel) and band-pass filtered between 1 Hz and 10 kHz. For both single-channel and multi-channel microelectrode recordings, the peak cathodic voltage at each recording location was calculated off-line by averaging peak voltages for 1 sec of recording data (i.e. 135 waveforms).

Because the impedance of the recording microelectrode can also influence the voltages measured in the brain, both DBS electrode and microelectrode impedances were monitored during the experiments. While DBS electrode impedances were measured at multiple time points during each experiment, the microelectrode impedance was monitored at the beginning and end of each experiment in order to ensure the microelectrode impedance remained stable throughout the duration of the experiment. Microelectrode impedances at 1 kHz were typically 0.5–1 M Ω . For both the DBS electrodes and recording microelectrodes, impedance measurements were performed at 1 kHz using a two-electrode configuration with an Autolab potentiostat (PGSTAT-12, Eco Chemie, Utrecht, The Netherlands) by applying a 25 mV (rms) sine wave between the working electrode (i.e. DBS contact or recording microelectrode) and a large surface area Ag|AgCl wire placed in the saline-filled contralateral access chamber. The current output was measured and the impedance was calculated in the frequency domain using Ohm's law. The animal's chair was grounded to help minimize the effects of surrounding noise.

2.2. Surgical procedure and DBS electrode implantation

The data presented in this study were acquired from three DBS electrodes chronically implanted in the brains of two rhesus macaque monkeys (8–10 years old; weighing 5–6 kg) following previously described surgical implant procedures (Elder et al., 2005; Miocinovic et al., 2007). The electrodes were implanted in regions of the brain that are common targets for treating movement disorders with DBS (i.e. thalamus, subthalamic nucleus (STN), and globus pallidus (GP)). All surgical and recording protocols were approved by the Cleveland Clinic Institutional Animal Care and Use Committee and complied with the United States Public Health Service policy on the humane care and use of laboratory animals.

2.3. Voltage changes after DBS electrode implantation

The effect of the foreign body reaction on the voltages generated in the brain during DBS was investigated by performing microelectrode recordings periodically after implantation. Microelectrode recordings during voltage-controlled DBS were acquired at multiple insertion locations parallel to the DBS electrode lead, and the peak recorded voltage was compared at one day and seven days after implantation. Two DBS electrodes implanted in the STN of one animal and the GP of a second animal were used in this analysis ($n = 6$, 3 contacts from each DBS lead) and the average peak voltages were determined from 10 recording locations centered around each DBS contact. The relative position of the DBS electrode and recording microelectrode was monitored with X-ray images during each experimental session (Fig. 1A).

2.4. Voltage changes during voltage-controlled DBS

Temporal fluctuations in the voltages generated in the brain during clinically-relevant, voltage-controlled DBS were examined with microelectrode recordings. DBS was applied for a total of 60 minutes and voltage recordings were obtained using a linear array of 8 microelectrodes. Multiple experiments ($n = 4$) were performed when applying stimulation through multiple contacts of a single DBS lead implanted in the thalamus and the peak voltages at each recording location of the microelectrode array were averaged.

2.5. Voltage-controlled v. current-controlled DBS

A separate set of experiments was also performed to examine differences in the temporal voltage fluctuations generated during voltage-controlled and current-controlled DBS. At the beginning of the experiment, a short duration (~one second) voltage-controlled stimulation train was applied through a DBS contact and the voltage generated in the brain was recorded with a single-channel microelectrode. After this brief voltage-controlled stimulation train, 60 minutes of current-controlled stimulation was applied through the same DBS contact, and the voltage measured at the adjacent microelectrode was again recorded. At the end of the 60 minutes of current-controlled DBS, an additional one second voltage-controlled stimulation train was applied and the voltage was measured at the same location. This experimental design provided a means to compare the effects of stimulation-induced changes at the electrode-tissue interface on the voltage distributions generated during voltage-controlled and current-controlled DBS. Three separate experiments were performed on multiple contacts from a single DBS lead implanted in the thalamus ($n=3$).

For all of the experimental situations described above, the Spearman rank correlation coefficient (r_s) was calculated in order to examine possible correlations between changes in the DBS electrode impedance and the voltages recorded in the brain.

3. Results

When comparing microelectrode voltage recordings of short periods of acute stimulation on day 1 to day 7 after chronic implantation of the DBS electrode, we observed an average decrease of $38.6 \pm 10.6\%$ in the peak cathodic voltage during voltage-controlled stimulation ($n = 6$) (Fig. 2). This voltage decrease was accompanied by a corresponding average increase in the 1 kHz DBS electrode impedance of $298 \pm 136\%$. The decrease in the peak cathodic voltage between day 1 and day 7 exhibited a strong negative correlation with the increase in the DBS electrode impedance ($r_s = -0.804$, $p = 9.65e-29$).

During experiments in which we applied continuous high frequency (135 Hz) DBS, there was a rapid decrease in the DBS electrode impedance during the first 10–15 minutes of stimulation that began to stabilize within the first hour of stimulation (Fig. 3A). During voltage-controlled DBS, voltage recordings from the tissue medium showed an increase in the peak cathodic

amplitude that followed a similar time scale (Fig. 3A). After 60 minutes of stimulation, there was an average decrease in the 1 kHz DBS electrode impedance of $47.9 \pm 16.7\%$ that coincided with an average increase in the peak recorded cathodic amplitude of $19.3 \pm 6.2\%$ ($n = 4$) (Fig. 3B). This increase in the peak voltage amplitude was negatively correlated with the measured decrease in 1kHz DBS electrode impedance ($r_s = -0.590$, $p = 4.42e-7$).

In a separate set of experiments, current-controlled DBS showed an average increase of only $6.5 \pm 1.1\%$ in the peak recorded cathodic amplitude after 1 hour of stimulation while voltage-controlled stimulation exhibited a larger and much more variable average change of $54.8 \pm 54.5\%$ ($n=3$) (Fig. 4). The average decrease in DBS electrode impedance for this set of experiments was $48.9 \pm 30.1\%$. The increase in the peak cathodic voltage recorded during voltage-controlled DBS was highly correlated with the decrease in DBS electrode impedance ($r_s = -0.927$, $p = 0.017$) while the voltage changes recorded during current-controlled DBS were not significantly correlated with the decrease in DBS electrode impedance ($r_s = 0.657$, $p = 0.175$).

4. Discussion

The goal of this study was to examine temporal fluctuations in the voltages generated in the brain during DBS and investigate potential advantages of current-controlled over voltage-controlled DBS. Our results show that (1) changes in the composition of the electrode-tissue interface after implantation produce an increase in DBS electrode impedance and a decrease in the voltage magnitudes generated in the brain by voltage-controlled DBS, (2) stimulation produces a decrease in DBS electrode impedance and a corresponding increase in the voltage magnitudes, and (3) the observed temporal voltage changes are reduced during current-controlled stimulation relative to voltage-controlled stimulation.

After an electrode is implanted into the nervous system, there is a foreign body reaction to the implanted device that results in the attachment of proteins and cells directly to the electrode contact and accumulation of extracellular matrix proteins and glia surrounding the device (Szarowski et al., 2003; Polikov et al., 2005; Anderson et al., 2008). These changes at the electrode-tissue interface appear as an increase in the electrode impedance (Williams et al., 2007; Lempka et al., 2009). Stimulation through a DBS electrode contact reverses some of these impedance changes induced by the foreign body reaction (Hemm et al., 2004; Lempka et al., 2009), which is noteworthy because these impedance changes may directly affect the voltage distributions generated in the brain.

The fundamental purpose of DBS is to modulate neural activity with electric fields, and as such, understanding the factors that affect the voltage distribution in the tissue medium have relevance to the clinical application of DBS, and in particular, the clinical programming of DBS systems. After a DBS system is surgically implanted, there is typically a period of time (~3–4 weeks) in which initial device programming is delayed (Deuschl et al., 2006). This delay provides an opportunity for microlesioning effects and local edematous changes to subside and the foreign-body reaction to stabilize. Fig. 2 shows that the changing electrode-tissue interface during this delay period can substantially alter the voltage magnitudes generated in the brain tissue during voltage-controlled DBS. As a result, stimulation parameters may require frequent adjustment if programming is performed during the first few weeks after DBS electrode implantation.

Voltage-controlled stimulation may also contribute to additional difficulties related to the identification of therapeutic stimulation parameter settings. Soon after clinical identification of an initial therapeutic stimulation setting, unwanted side effects (e.g. muscle contractions, dyskinesias, and paresthesias) can gradually appear over ~1–2 hours of continuous stimulation.

The results presented in this study suggest the appearance of these unwanted side effects are due in part to the decrease in the electrode impedance during stimulation and the corresponding increase in the voltage magnitudes generated in the neural tissue (Fig. 3). Such alterations likely cause the stimulation to activate a larger volume of tissue that may include brain regions responsible for the appearance of such side effects (Butson et al., 2006).

The utilization of current-controlled DBS should minimize voltage fluctuations generated by impedance changes and may help reduce the amount of time required for patient programming. Our results show that voltage distributions generated during current-controlled stimulation are minimally affected by varying DBS electrode impedance conditions (Fig. 4). Therefore, changes in therapeutic outcome observed during patient programming with current-controlled DBS would not be contaminated by stimulation induced changes at the electrode-tissue interface that may occur over time. As an alternative, it should also be noted that one could minimize the consequences of using voltage-controlled DBS systems by first applying DBS at the contact of interest for an initial period (~30 minutes) to induce the major component of the decrease in the electrode impedance (Fig. 3A). Clinical programming performed immediately after this initial stimulation phase would only be subjected to relatively small changes in the electrode impedance.

Clinical and/or electrophysiological research studies characterizing the wash-in or wash-out effects of DBS with voltage-controlled stimulation also need to be cognizant of the electrode impedance and voltage fluctuations that occur following device activation. For example, recent interest has focused on studying modulation of beta-band activity in the STN immediately following DBS by recording local field potential activity through the DBS electrode (e.g. Kuhn et al., 2008; Bronte-Stewart et al., 2009). Electrode impedance fluctuations need to be considered in these types of experiments because the stimulation induced impedance changes at the active electrode contact(s) could affect the frequency content of the recorded neural signals through those contacts. These effects would be time dependent because the electrode impedance would rapidly decrease during stimulation and immediately begin to increase once stimulation is turned off. For the DBS electrodes examined in this study, electrode impedance began to rebound immediately after stimulation was turned off and often returned to pre-stimulation baseline levels within 1–2 days (data not shown). Other clinical experiments in which voltage-controlled DBS is turned off for many hours before the start of the experiment and then turned on to address clinical efficacy at a given parameter setting (e.g. Lopiano et al., 2003), should be aware that the first ~1 hour of data collection would be contaminated by the decreasing electrode impedance, increasing voltage distribution, and the subsequent non-stationary volume of stimulation. These impedance fluctuations are also important to consider during animal studies examining the therapeutic mechanisms of DBS in which stimulation is typically not chronic but only performed during the experiment and a variety of voltage-controlled stimulation parameter settings are examined within a short period of time (e.g. Hashimoto et al., 2003; Johnson et al., 2009).

While we believe the results of this study to be highly relevant to the field of deep brain stimulation and neurostimulation in general, this study was subject to a number of limitations. For example, although the results presented in this study suggest potential clinical advantages with current-controlled stimulation, these experiments were performed in an animal model and can only provide a hypothetical framework for future studies in human DBS patients. Further, generalization of the results presented in this study may also be limited because of the small number of animals used in these experiments.

Another potential limitation of this study was modifications to the voltage waveform profiles recorded in the tissue from various extraneous factors. One of these factors was the bandpass filtering of the recordings that produced significant distortions in both the low and high

frequency components of the recorded waveforms. In spite of these distortions produced from filtering, the shapes of the recorded waveforms were indicative of the system elements that were significantly contributing to the overall electrode impedance. For voltage-controlled stimulation, experimental situations were encountered in which the shape of the voltage waveform produced in the brain tissue during stimulation was dominated by the DBS electrode impedance and other instances in which the waveform shape was dominated by the tissue capacitance. For high electrode impedances ($>10\text{ k}\Omega$), the waveform shape was often dominated by the electrode capacitance and exhibited a peak at the beginning of the cathodic pulse and an exponential decay over the duration of the cathodic pulse (gray-dashed line at day 7 in Fig. 1B and the black line at 0 min in Fig. 4A). For low electrode impedances ($<10\text{ k}\Omega$), the waveform shape was often dominated by the tissue capacitance and exhibited an exponential increase in the cathodic voltages throughout the duration of the cathodic pulse (black line at day 1 in Fig. 1B and the gray-dashed line in Fig. 4A). For current-controlled stimulation, the shape of the voltage waveform generated in the brain was independent of the DBS electrode impedance and showed an exponential increase in the voltage due to tissue capacitance (Fig. 1B and Fig. 4A).

The shape of the voltage waveforms generated in the brain may also have been altered by the non-ideal behavior of the Medtronic IPG used to apply voltage-controlled stimulation in the described experiments. The IPG stimulation waveforms were not truly voltage-controlled, but applied stimulation via an output capacitor that was charged through charge pump circuitry. Because the IPG was not an ideal voltage source, variations in the DBS load impedance likely produced differences in the amplitude and/or time course of the stimulus waveform generated at the IPG output. To investigate these potential changes, the IPG output was measured for a range of experimentally-relevant load impedances (i.e. 1–30 k Ω). Differences in the amplitude and time course of the IPG output were observed for this range of impedances, however, these differences were very small relative to the voltage changes recorded in the tissue during the described experiments (data not shown).

In this study, the relationship between changes in DBS electrode impedance and the corresponding voltage distribution generated in the brain was quantified using the Spearman's rank-order correlation coefficient. The results of this study suggest that the DBS electrode impedance strongly affects the corresponding voltages generated in the brain during voltage-controlled DBS. However, it is important to keep in mind that there are possible extraneous variables (e.g. differences between animals, individual DBS contacts, electrode location, and the relative distance between the DBS contact and individual microelectrode recording locations) that were not accounted for in this analysis.

This study utilized experimental techniques to monitor the temporal evolution of the voltage distribution generated in the brains of non-human primates during DBS. Our results show that substantial variability in extracellularly recorded voltages can occur during voltage-controlled DBS due to variable DBS electrode impedance conditions. Such changes can directly affect the volume of neural tissue activated during stimulation (Butson et al., 2006). In contrast, current-controlled DBS produced minimal changes in the voltage distribution generated in the brain even with large decreases in electrode impedance. Therefore, current-controlled DBS should be considered as a way to minimize variability in the spread of stimulation for a given set of stimulation parameter settings. In turn, adoption of current-controlled DBS should provide three advantages over voltage-controlled DBS: 1) enable more consistent comparison of parameter settings within and across patients, 2) reduce confounding variables when researching the time-dependent behavioral and/or electrophysiological effects related to the onset of DBS, and 3) provide a more consistent stimulation effect during the initial clinical programming process.

Acknowledgments

The authors would like to thank Gary Russo, Weidong Xu, and Jianyu Zhang for their help with experimental preparations and Jennie Minnich for assistance in animal care. This research was supported by the National Institutes of Health (R01 NS047388, R01 NS037019, and F32 NS061541) and by a United States Department of Education Graduate Assistance in the Areas of National Need (GAANN) fellowship.

References

- Anderson JM, Rodriguez A, Chang DT. Foreign body reaction to biomaterials. *Semin Immunol* 2008 Apr;20(2):86–100. [PubMed: 18162407]
- Bronte-Stewart H, Barberini C, Koop MM, Hill BC, Henderson JM, Wingeier B. The STN beta-band profile in Parkinson's disease is stationary and shows prolonged attenuation after deep brain stimulation. *Exp Neurol* 2009 Jan;215(1):20–28. [PubMed: 18929561]
- Butson CR, Maks CB, McIntyre CC. Sources and effects of electrode impedance during deep brain stimulation. *Clin Neurophysiol* 2006 Feb;117(2):447–454. [PubMed: 16376143]
- Deuschl G, Herzog J, Kleiner-Fisman G, Kubu C, Lozano AM, Lyons KE, et al. Deep brain stimulation: postoperative issues. *Mov Disord* 2006 Jun;21(Suppl 14):S219–237. [PubMed: 16810719]
- Elder CM, Hashimoto T, Zhang JY, Vitek JL. Chronic implantation of deep brain stimulation leads in animal models of neurological disorders. *Journal of Neuroscience Methods* 2005 Mar 15;142(1):11–16. [PubMed: 15652612]
- Hashimoto T, Elder CM, Okun MS, Patrick SK, Vitek JL. Stimulation of the subthalamic nucleus changes the firing pattern of pallidal neurons. *J Neurosci* 2003 Mar 1;23(5):1916–1923. [PubMed: 12629196]
- Hemm S, Vayssiere N, Mennessier G, Cif L, Zanca M, Ravel P, et al. Evolution of brain impedance in dystonic patients treated by GPi electrical stimulation. *Neuromodulation* 2004 Apr;7(2):67–75.
- Johnson MD, Vitek JL, McIntyre CC. Pallidal stimulation that improves parkinsonian motor symptoms also modulates neuronal firing patterns in primary motor cortex in the MPTP-treated monkey. *Exp Neurol* 2009 Sep;219(1):359–362. [PubMed: 19409895]
- Kühn AA, Kempf F, Brücke C, Gaynor Doyle L, Martinez-Torrez I, Pogosyan A, et al. High-frequency stimulation of the subthalamic nucleus suppresses oscillatory beta activity in patients with Parkinson's disease in parallel with improvement in motor performance. *J Neurosci* 2008 Jun 11;28(24):6165–6173. [PubMed: 18550758]
- Lempka SF, Miocinovic S, Johnson MD, Vitek JL, McIntyre CC. In vivo impedance spectroscopy of deep brain stimulation electrodes. *J Neural Eng* 2009 Jun 3;6(4):46001.
- Lopiano L, Torre E, Benedetti F, Bergamasco B, Perozzo P, Pollo A, et al. Temporal changes in movement time during the switch of the stimulators in Parkinson's disease patients treated by subthalamic nucleus stimulation. *Eur Neurol* 2003;50(2):94–99. [PubMed: 12944714]
- Miocinovic S, Lempka SF, Russo GS, Maks CB, Butson CR, Sakaie KE, et al. Experimental and theoretical characterization of the voltage distribution generated by deep brain stimulation. *Exp Neurol* 2009 Mar;216(1):166–176. [PubMed: 19118551]
- Miocinovic S, Zhang J, Xu W, Russo GS, Vitek JL, McIntyre CC. Stereotactic neurosurgical planning, recording, and visualization for deep brain stimulation in non-human primates. *J Neurosci Methods* 2007 May 15;162(1–2):32–41. [PubMed: 17275094]
- Perlmutter JS, Mink JW. Deep brain stimulation. *Annu Rev Neurosci* 2006;29:229–257. [PubMed: 16776585]
- Polikov VS, Tresco PA, Reichert WM. Response of brain tissue to chronically implanted neural electrodes. *J Neurosci Methods* 2005 Oct 15;148(1):1–18. [PubMed: 16198003]
- Szarowski DH, Andersen MD, Retterer S, Spence AJ, Isaacson M, Craighead HG, et al. Brain responses to micro-machined silicon devices. *Brain Res* 2003 Sep 5;983(1–2):23–35. [PubMed: 12914963]
- Williams JC, Hippensteel JA, Dilgen J, Shain W, Kipke DR. Complex impedance spectroscopy for monitoring tissue responses to inserted neural implants. *J Neural Eng* 2007 Dec;4(4):410–423. [PubMed: 18057508]

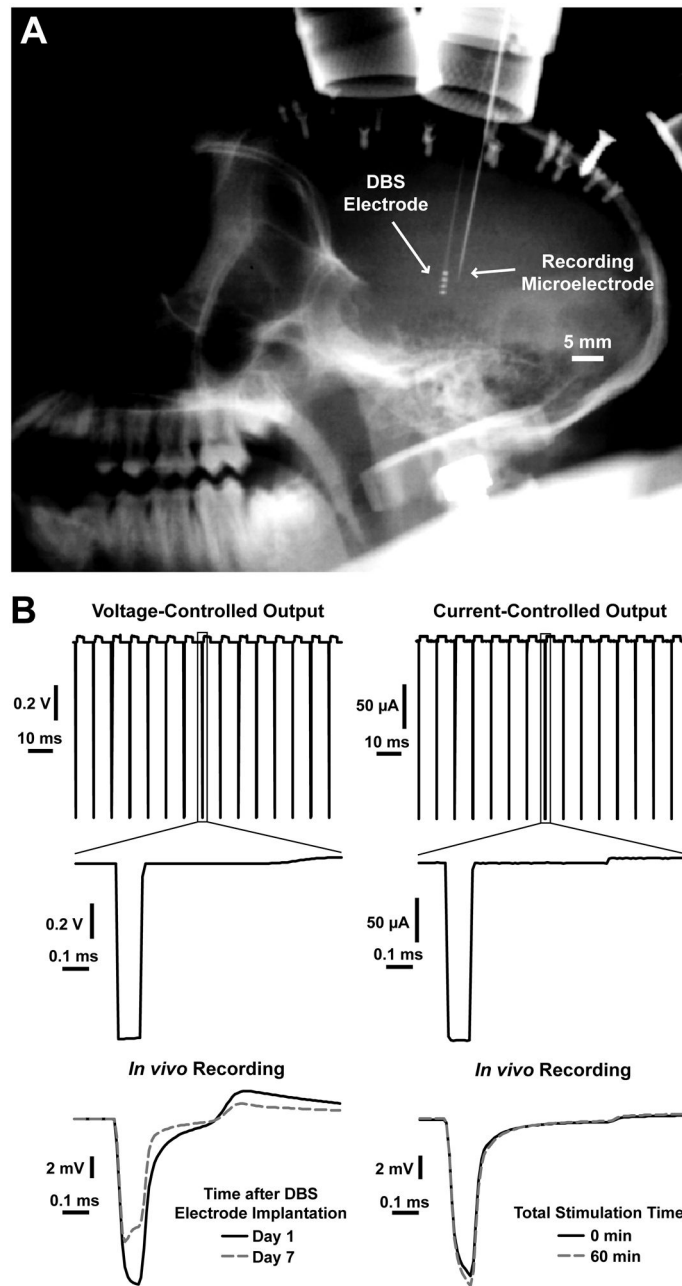


Fig. 1.

In vivo microelectrode recordings examining the temporal evolution of the voltages generated in the brain during DBS. (A) X-ray image showing a chronically-implanted DBS electrode and an acutely-inserted recording microelectrode used to monitor the voltages generated in the brain during DBS. The recording electrode was inserted approximately 2 mm away from the DBS lead. (B) Recordings of the voltage-controlled and current-controlled stimulus waveforms examined in this study and examples of the voltage waveforms recorded in the brain tissue. The example of *in vivo* voltages recorded during voltage-controlled stimulation is from one of the recording locations shown in Fig. 2A and shows the changes that occur during the first week after DBS electrode implantation. The example recordings for current-controlled stimulation show the small changes that occur during one hour of stimulation.

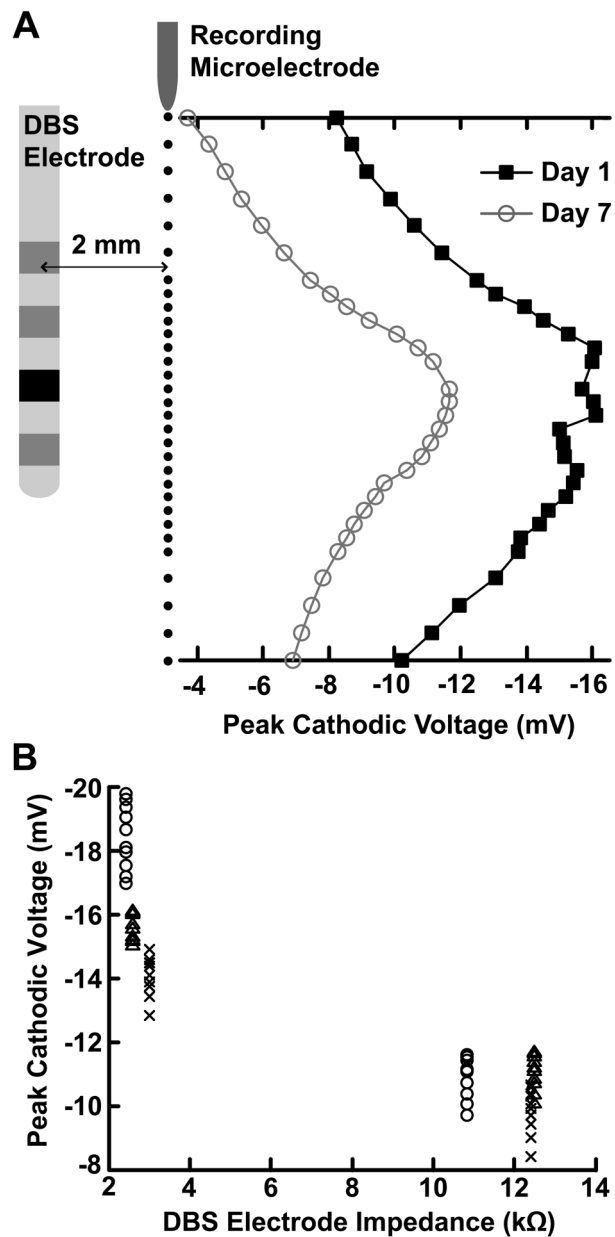


Fig. 2. Effect of the foreign-body reaction on the voltages generated in the brain during voltage-controlled DBS. (A) Microelectrode recordings were performed 1 day and 7 days after implantation of the DBS electrode at the locations indicated by the linear array of black dots parallel to the electrode. The plotted values display an example of the average peak cathodic voltages measured during voltage-controlled stimulation 1 day and 7 days after implantation for the DBS contact shown in black. (B) Plots of the DBS electrode impedance versus the peak cathodic voltages recorded 1 day and 7 days after implantation for the DBS lead implanted in the STN. Each marker type (i.e. circle, triangle, cross) correspond to an individual DBS contact. Between 1 day and 7 days after implantation, there was a $38.3 \pm 10.5\%$ decrease in the peak cathodic voltage and a corresponding average increase in the 1 kHz DBS electrode impedance of $298 \pm 136\%$ ($n=6$). The decrease in the peak cathodic voltage exhibited a strong negative correlation with the increase in the DBS electrode impedance ($r_s = -0.803$, $p = 2.61e-28$). Ten

recording locations centered around each DBS contact were used in this analysis (see Methods), corresponding to ten peak voltage measurements for each DBS electrode impedance.

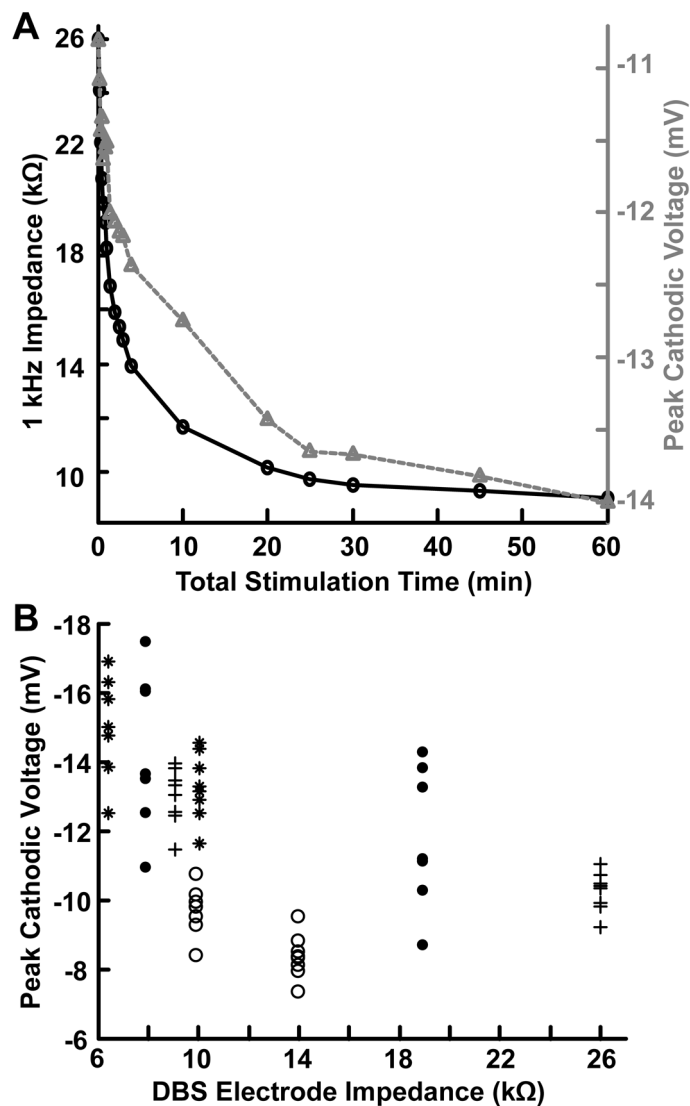


Fig. 3. Temporal voltage fluctuations observed in the brain during voltage-controlled DBS. (A) Double y-axis plot showing an example of the temporal changes in both the 1 kHz impedance of the DBS electrode and the peak cathodic voltages during one hour of voltage-controlled DBS. The black line and circle markers indicate the 1 kHz impedance of the DBS electrode and the gray dashed line and triangle markers indicate the peak cathodic voltages. (B) Plot of the DBS electrode impedance versus the peak cathodic voltages recorded after 0 and 60 minutes of stimulation. Each marker type (e.g. circle, asterisk) corresponds to an individual experiment. After 60 minutes of stimulation, there was an average decrease in the 1 kHz DBS electrode impedance of $47.9 \pm 16.7\%$ that coincided with an average increase in the peak recorded cathodic amplitude of $19.3 \pm 6.2\%$ ($n = 4$). This increase in the peak voltage amplitude was negatively correlated with the measured decrease in 1kHz DBS electrode impedance ($r_s = -0.590$, $p = 4.42e-7$). Voltages for this set of experiments were recorded with an eight-contact microelectrode array (see Methods), corresponding to eight peak voltage measurements for each DBS electrode impedance.

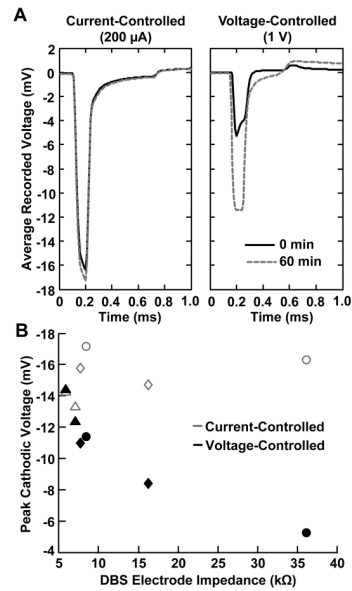


Fig. 4.

Temporal voltage changes observed during current-controlled and voltage-controlled DBS. (A) Microelectrode recordings of the voltages generated in the brain during current-controlled and voltage-controlled DBS. The black line represents the stimulus waveform recorded at the beginning of stimulation and the gray-dashed line represents the stimulus waveform recorded after one hour of stimulation. (B) Plot of the DBS electrode impedance versus the peak cathodic voltages recorded during current-controlled (gray markers) and voltage-controlled (black markers) stimulation. Each marker type corresponds to an individual experiment (i.e. triangle, square, and circle). Current-controlled DBS showed an average increase of only $6.5 \pm 1.1\%$ in the peak recorded cathodic amplitude after 1 hour of stimulation while voltage-controlled stimulation exhibited a larger and much more variable average change of $54.8 \pm 54.5\%$ ($n=3$) (Fig. 4). The average decrease in DBS electrode impedance for this set of experiments was $48.9 \pm 30.1\%$. The increase in the peak cathodic voltage recorded during voltage-controlled DBS was highly correlated with the decrease in DBS electrode impedance ($r_s = -0.927$, $p = 0.017$) while the voltage changes recorded during current-controlled DBS were not significantly correlated with the decrease in DBS electrode impedance ($r_s = 0.657$, $p = 0.175$).